



OPEN

Convolutional neural networks for approximating electrical and thermal conductivities of Cu-CNT composites

Faizan Ejaz¹, Leslie K. Hwang², Jangyup Son^{3,4}, Jin-Sang Kim⁵, Dong Su Lee³ & Beomjin Kwon¹✉

This article explores the deep learning approach towards approximating the effective electrical and thermal conductivities of copper (Cu)-carbon nanotube (CNT) composites with CNTs aligned to the field direction. Convolutional neural networks (CNN) are trained to map the two-dimensional images of stochastic Cu-CNT networks to corresponding conductivities. The CNN model learns to estimate the Cu-CNT composite conductivities for various CNT volume fractions, interfacial electrical resistances, $R_c = 20 \Omega - 20 \text{ k}\Omega$, and interfacial thermal resistances, $R''_{t,c} = 10^{-10} - 10^{-7} \text{ m}^2\text{K/W}$. For training the CNNs, the hyperparameters such as learning rate, minibatch size, and hidden layer neurons are optimized. Without iteratively solving the physical governing equations, the trained CNN model approximates the electrical and thermal conductivities within a second with the coefficient of determination (R^2) greater than 98%, which may take longer than 100 min for a convectional numerical simulation. This work demonstrates the potential of the deep learning surrogate model for the complex transport processes in composite materials.

Copper (Cu) is by far the most widely used conductive material in electronics, aviation, construction and power transmission lines. The progressive miniaturization and sophistication of high-power density devices demand copper alternatives to facilitate efficient electrical and thermal transport. Cu-carbon nanotube (CNT) composites are theoretically estimated to be superior electrical and thermal conductors to Cu at room temperature (27 °C)¹. The conductivities of Cu-CNT composites are strongly influenced by CNT morphologies, i.e., CNT volume fraction and interfacial resistance at Cu-CNT and CNT-CNT interfaces. The electrical and thermal transport in CNT composites manifests in complex physics, which is extremely challenging to represent with closed-form models. Existing physics-based models, e.g., finite element model (FEM), are highly compute intensive, predominantly due to the extremely fine mesh required for CNTs and CNT-CNT interfaces.

Deep learning, a class of machine learning (ML), is applied in various scientific research areas to readily discover features from high-dimensional unstructured data (e.g., images, audio clips)^{2,3}. For some nonlinear transport problems accompanied with complex physics in composites, deep learning algorithms interpret nonlinear patterns of data to classify or predict outputs without iteratively calculating the governing physical equations; thus, demanding lower computational costs than numerical simulation techniques⁴⁻⁸. Thus, researchers are actively investigating data driven deep learning analysis as an alternate modeling approach in composites⁹⁻¹².

With the recent rapid development of ML methods, there has been growing interest in predicting the nano-composite attributes without performing compute-intensive simulations. A previous study used convolutional neural networks (CNN) to predict thermal conductivity in composite materials⁹. 1500 composite material structures with volume fractions up to 30% were generated using the quartet structure generation set and effective thermal conductivities were calculated using the lattice Boltzmann method (LBM). The predicted results using CNN were found close to LBM with root mean square error (RMSE) of 1.9%. A past study utilized artificial neural networks (ANN) to determine the most favorable bridging alloying atom in Aluminum-CNT composite¹⁰.

¹School for Engineering of Matter, Transport and Energy, Arizona State University, Tempe, AZ 85287, USA. ²Independent researcher, Chandler, Arizona, USA. ³Functional Composite Materials Research Center, Korea Institute of Science and Technology (KIST), Jeonbuk 55324, Republic of Korea. ⁴Division of Nano and Information Technology, KIST School University of Science and Technology (UST), Jeonbuk 55324, Republic of Korea. ⁵Institute of Advanced Composite Materials, Korea Institute of Science and Technology, Jeonbuk 55324, Republic of Korea. ✉email: kwon@asu.edu

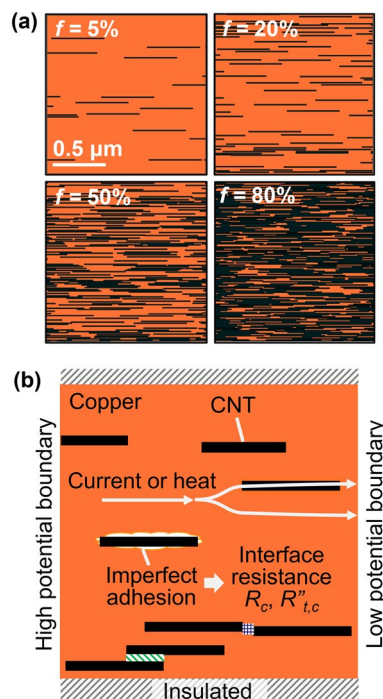


Figure 1. (a) Schematics of Cu-CNT networks with various CNT fractions f , (b) Schematic of a Cu-CNT network with boundary conditions. The patterned bars represent the side-to-side and end-to-end CNT-CNT interfacial resistance.

ANN was trained with 357 examples from literature for various alloying elements along with their strengthening efficiencies. The strengthening efficiencies approximated by the ML model were comparable to those of experiments with accuracy greater than 90%. Another research used ANN to predict the multiaxial strain-sensing response of CNT-polymer composites¹¹. The ML model employed physics-based FEM at microscale to generate 15,000 examples to train ANN and approximated the macro-scale strain responses in CNT-polymer composites with accuracy of 99.65%. One previous record developed and trained the Gaussian Process Regression (GPR) model to predict the tensile strength in CNT-polymers nanocomposites¹². The training data was collected from the available literature with 23 different polymers, combined with 22 CNT incorporating methods and 20 CNT modifications. The GPR model exhibited strong performance in predicting the tensile strength of CNT-polymer composites with training and validation accuracy of greater than 91%.

In this article, a convolutional neural network (CNN) is presented that infers the electrical and thermal conductivity of Cu-CNT composites at room temperature (27 °C) when an input data describing the stochastic distribution of CNTs, CNT volume fraction and Cu-CNT interfacial resistance is provided. The CNN model learns the important features from the images of Cu-CNT networks to predict the conductivities. To improve the accuracy of the CNN model, the influence of various hyperparameters such as learning rate, batch size and number of neurons in hidden layers is investigated. The trained CNN can serve as a surrogate model for Cu-CNT composite systems if the morphology of CNT network can be expressed in two-dimensional (2D) image format. For example, if the 2D images of Cu-CNT composites that sharply visualize the boundaries of CNTs, obtained either from computational modeling or processed microscopic images, are available, the trained CNN can rapidly examine the composite properties before conducting the expensive FEM or actual measurements.

Training data generation

Training data is generated by creating the 2D stochastic Cu-CNT networks and simulating their electrical and thermal conductivities. A 2D finite element model (FEM) is used for the simulation that accounts for the CNT volume fractions, f , Cu-CNT interfacial resistances, and CNT-CNT interfacial resistances arising from the van der Waals interaction between two closely spaced CNTs. Since full details of FEM are available elsewhere¹³, only a minimal description follows. The 2D FEM model employs a simplified CNT morphology, i.e., straight CNTs aligned to the field direction, enabling the simulations of CNT networks with high volume fractions (up to 80%) at reduced computational costs. Several studies have reported that aligned, straightened CNTs exhibit enhanced electrical and thermal conductivities than entangled, randomly oriented CNTs^{14–18}. Figure 1a illustrates some examples of Cu-CNT network models with various f . The 2D composite consists of non-overlapping CNTs (length 500 nm and width 10 nm) which are randomly distributed in the Cu matrix. Figure 1b shows the electrical and thermal boundary conditions used in FEM, which represent the following configurations: (1) steady-state electrical conduction and (2) heat conduction without internal heat generation. For electrical analysis, a potential difference, ΔV , of 1 μV is applied across the domain of length, L . For thermal analysis, the

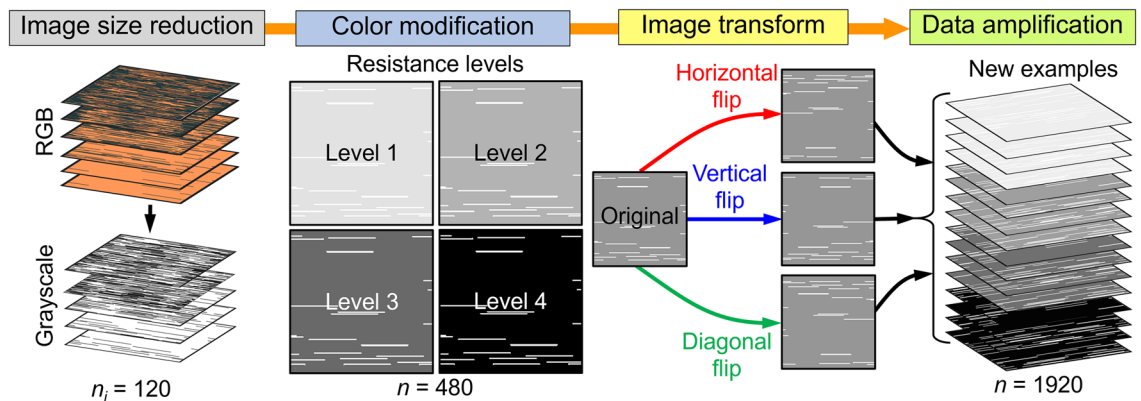


Figure 2. Schematic for the data preparation. The image data size of Cu-CNT networks is reduced by converting RGB scale into grayscale. The Cu-CNT interfacial resistance is encoded by the selection of Cu domain color intensity. The resistance levels are defined as follows. Level 1: $R_c = 20 \text{ k}\Omega$ or $R''_{t,c} = 10^{-7} \text{ m}^2\text{K/W}$, Level 2: $R_c = 2 \text{ k}\Omega$ or $R''_{t,c} = 10^{-8} \text{ m}^2\text{K/W}$, Level 3: $R_c = 200 \Omega$ or $R''_{t,c} = 10^{-9} \text{ m}^2\text{K/W}$, and Level 4: $R_c = 20 \Omega$ or $R''_{t,c} = 10^{-10} \text{ m}^2\text{K/W}$. The images are flipped horizontally, vertically, and diagonally to amplify the training dataset by four folds.

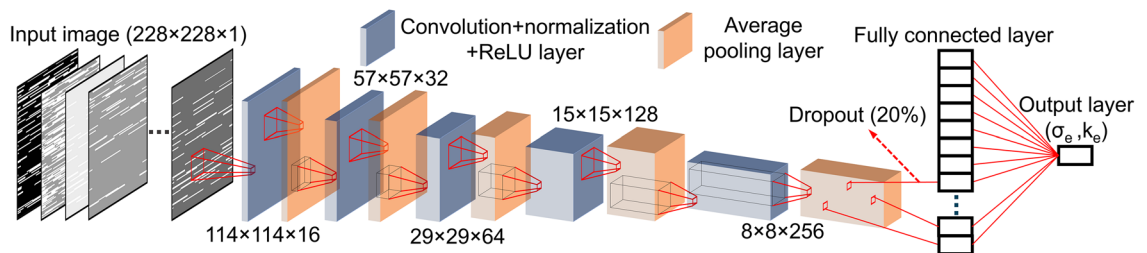


Figure 3. The architecture of CNN to approximate the effective electrical and thermal conductivities of Cu-CNT networks. σ_e denotes the effective electrical conductivity and k_e denotes the effective thermal conductivity.

initial domain temperature is set to 27°C and the temperature difference across the domain, ΔT , is kept at 1°C . At Cu-CNT interfaces, the interfacial electrical resistance (R_c) and interfacial thermal resistance ($R''_{t,c}$) are defined in the ranges of $R_c = 20 \Omega - 20 \text{ k}\Omega$ and $R''_{t,c} = 10^{-10} - 10^{-7} \text{ m}^2\text{K/W}$. The FEM estimates the electrical potential and temperature distributions in the Cu-CNT composite that are needed for the computation of effective electrical conductivity (σ_e) and thermal conductivity (k_e). The conductivities are normalized by the Cu matrix electrical conductivity ($\sigma_{Cu} = 0.58 \times 10^8 \text{ S/m}$)¹³ and thermal conductivity ($k_{Cu} = 401 \text{ W/mK}$)¹³ at room temperature.

The training dataset is collected using FEM simulations and data augmentation. Figure 2 summarizes the data preparation process. First, 20 different images of Cu-CNT networks with random CNT distributions were generated for each target CNT fraction. Since 6 CNT volume fractions (i.e., $f = 5\%$, 10% , 20% , 50% , 70% and 80%) were considered, in total, 120 Cu-CNT network images were created. Three-channel RGB images of Cu-CNT networks were converted into single-channel gray images to reduce the size of data. The information of Cu-CNT interfacial resistance was encoded in the Cu-CNT network image through a color code. The color intensity of the Cu domain was chosen by assigning grayscale intensities representing R_c or $R''_{t,c}$, while the CNT regions were represented by white color (i.e., pixel intensity of 255). The pixel intensity of the Cu domain was varied as 0, 63, 129, 163 to encode four different levels of R_c and $R''_{t,c}$. The total number of images after the color modification is increased to 480. The amount of training data was amplified using a simple image transformation technique, similar to a previous work⁴. As shown in Fig. 2, the original images were flipped in three ways: (1) horizontal, (2) vertical and (3) diagonal flips. The transformed Cu-CNT networks were assumed to possess identical conductivities to their original Cu-CNT network. With the data augmentation, the total number of Cu-CNT network models is increased to 1920. Finally, the Cu-CNT network images and tabulated electrical and thermal conductivities from FEM simulations were paired as the training dataset.

Convolutional neural network

Convolutional neural network (CNN) is a class of deep neural networks which is widely-used in image recognition tasks with remarkable success¹⁹. There are several CNN models with different structures successfully applied for image recognition such as AlexNet²⁰, ResNet²¹, LeNet-5²², etc. The CNN model outperforms other machine learning algorithms in terms of non-linear function approximation and the ability to extract and articulate data features²³. Thus, compared to conventional artificial neural networks such as multilayer perceptron and feed-forward networks, the CNN significantly reduces the computational demands when processing high-dimensional image information due to the feature parameter sharing and dimensionality reduction. Figure 3 shows the

Case	Neurons in each layer	σ_e/σ_{Cu} predictions			k_e/k_{Cu} predictions		
		R^2_{Train}	R^2_{Valid}	Time (s)	R^2_{Train}	R^2_{Valid}	Time (s)
1	10, 20, 30, 40, 50, 60	0.83	0.79	110	0.83	0.71	114
2	20, 40, 60, 80, 100, 120	0.87	0.86	144	0.89	0.87	152
3	40, 80, 120, 160, 200, 240	0.96	0.91	280	0.94	0.90	299
4	8, 16, 32, 64, 128, 256	0.99	0.98	170	0.99	0.98	175
5	16, 32, 64, 128, 256, 512	0.99	0.94	352	0.98	0.92	322

Table 1. CNN model R^2 and training time obtained with various hidden layer neurons.

architecture of our CNN model obtained through hyperparameter tuning which is discussed in the next section. The CNN model consists of an input layer (i.e., Cu-CNT network), an output layer (i.e., predicted conductivities) and 6 hidden layers. The input layer is a single channel Cu-CNT network image, equivalent to a $228 \times 228 \times 1$ matrix. The image size was chosen to retain high resolution and capture minuscule details of CNT networks, particularly at high CNT fractions. A convolution layer is added to generate feature maps from the input layer. The convolutional layer contains a series of 3×3 kernels which are convoluted with inputs to extract features while preserving the spatial relationships between image pixels. The batch normalization layer is added after every convolution layer to normalize and standardize the inputs between 0 and 1. A rectified linear unit activation (ReLU) layer is added to prevent the vanishing gradient problem, allowing the model to learn faster with improved stability. To down-sample the input feature map, a pooling layer with a filter size of 2 and stride of 2 is inserted after every activation layer. The pooling layer applies an average pooling operation in a prescribed filter size and abstracts the input feature maps, reducing the low-level features while extracting high-order features. After 6 iterations of hidden layers, a fully connected layer takes all the outputs in the previous layer and connects them to its single neuron, i.e., a one-dimensional feature vector. The feature vector represents the major features of the original input and can be used to establish the regression model for the electrical or thermal conductivities.

To train the CNN model, stochastic gradient descent (SGD) algorithm is used. SGD is one of the popular iterative optimization techniques for determining weights that minimize the errors in neural networks. SGD calculates the gradients on small randomized subsets of the training set, called minibatch. The gradient is calculated in small-steps called learning rate which determines the moving step size from one point to the next point with a negative gradient. After a full forward and backward pass on the complete training dataset, i.e., 1 epoch, the model weights are updated. By testing with a minibatch in the range of 5–20 and learning rate in the range of 10^{-2} – 10^{-7} , we selected an optimal minibatch size as 20, a learning rate as 10^{-3} and epochs as 400. The learning rate was dropped by a factor of 0.1 after every 150 epochs, allowing the model to learn an optimal set of weights. The model training begins by initiating the kernel parameters using Gaussian initialization method which extracts the features of the Cu-CNT network. The kernel parameters are optimized according to the Euclidean loss function, $(1/n) \sum_{i=1}^n \|y_i - y_i'\|^2$, which calculates the square sum of the difference between the two training outputs, i.e., predictive value, y_i and known value, y_i' . The loss function is subsequently minimized after each iteration by updating the parameters.

Results and discussion

The number of neurons in hidden layers was adjusted to balance the model accuracy and training time. The coefficient of determination (R^2) was employed to quantitatively examine the model accuracy. Table 1 summarizes the R^2 of training dataset (R^2_{Train}) and the validation dataset (R^2_{Valid}) along with model training time as a function of neurons in each convolution layer for both σ_e/σ_{Cu} and k_e/k_{Cu} predictions. The model training was performed on a graphic card (Nvidia RTX A6000) with 48 GB memory. In general, as the number of neurons, equivalently the depth of output volume, increases, both training and validation R^2 increases along with the cost of additional training time. In our experiment, the number of neurons used in case 4 provided the highest R^2_{Train} and R^2_{Valid} (≥ 0.98) with a training time of ~ 3 min. The model R^2 was not improved by further increasing the number of neurons as seen in case 5. Therefore, the number of neurons in each layer was chosen to be 16, 32, 64, 128 and 256 for all subsequent CNN training.

The CNN was trained to predict the electrical and thermal conductivities of the Cu-CNT networks over wide range of interfacial resistances, i.e., $R_c = 20 \Omega$ – $20 \text{ k}\Omega$ and $R''_{tc} = 10^{-10} \text{ m}^2\text{K/W}$ – $10^{-7} \text{ m}^2\text{K/W}$. Figure 4 compares the CNN model approximations and FEM predictions for σ_e/σ_{Cu} and k_e/k_{Cu} . Overall, the training of CNN was successful with $R^2_{Train} \geq 0.99$, and the trained CNN was able to accurately predict the unseen Cu-CNT network models with $R^2_{Valid} \geq 0.98$. Note that training the CNN with 1920 Cu-CNT models took only ~ 3 min. With this training cost, the CNN model can estimate the conductivity of an unseen Cu-CNT network within 1 s, whereas the FEM requires ~ 155 min on average for the same task. Such characteristics of the CNN model suggest that the deep learning approach is a promising method when it is necessary to rapidly and repetitively estimate the properties of stochastic composite materials if the training dataset, i.e., images of composite materials and corresponding properties, is available.

The training and validation datasets were designed to include diversified examples with various CNT fractions and interfacial resistances. The diversity in training data critically affects whether the neural network is able to overcome the bias or not. In our dataset, σ_e/σ_{Cu} ranges from 0.08 to 10.45 and k_e/k_{Cu} ranges from 0.15 to 4.25 as shown in Fig. 4. For the data generated with a large interfacial resistance (i.e., $R_c = 20 \text{ k}\Omega$ and $R''_{tc} = 10^{-7} \text{ m}^2\text{K/W}$), the Cu-CNT composites with high f (i.e., $f \geq 50\%$) possessed effective conductivities that were smaller than that

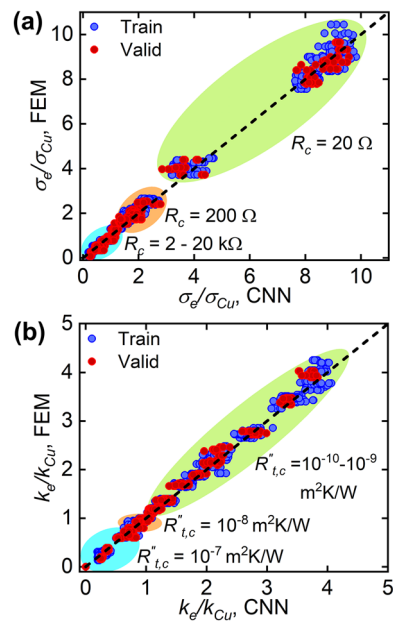


Figure 4. Comparison between CNN approximations and FEM predictions for (a) effective electrical conductivities with $R^2_{\text{Train}} = 0.991$, $R^2_{\text{Valid}} = 0.982$, and (b) effective thermal conductivities with $R^2_{\text{Train}} = 0.992$, $R^2_{\text{Valid}} = 0.986$.

of copper (i.e., $0 < \sigma_e/\sigma_{Cu}$, $k_e/k_{Cu} < 0.5$). For the examples with a large R_c , R''_{tc} and small f (i.e., $f < 20\%$), the effective conductivities were close to unity. When the interfacial resistance is small (i.e., $R_c = 20 \Omega$ and $R''_{tc} = 10^{-10} \text{ m}^2\text{K/W}$), the examples with high f (i.e., $f \geq 50\%$) exhibited effective conductivities that were greater than that of copper (i.e., $7.5 < \sigma_e/\sigma_{Cu} < 11$ and $2 < k_e/k_{Cu} < 4.5$). By combining various levels of f , R_c and R''_{tc} , the dataset incorporated the examples having effective conductivities similar to previously reported Cu-CNT composites^{24–31}.

The method introduced in this article demonstrates that the deep neural networks can rapidly approximate the complex relation between the morphology of fiber composites and their electrical and thermal transport properties. The introduced approach will be useful for the researchers who need a surrogate model for fiber composite systems that estimates the composite properties before the expensive finite element simulations or actual measurements. Thus, the application of the introduced approach for inferring the properties of actual composite materials can be an extension of this work. Since the images of Cu-CNT composites used in this work showed the shapes of CNTs distinctly without any blurriness, the CNN readily recognized the layouts of CNTs and made predictions accurately. For the application of the introduced approach to actual materials, it will be necessary to acquire microscopic images of the samples from various parts and process the images to extract the morphology of CNT network similar to Fig. 1a while eliminating the background image features.

Conclusions

This work reports a CNN that is trained to approximate the effective electrical and thermal conductivities of stochastic Cu-CNT networks when their 2D images are provided as inputs. The CNN architecture and hyperparameters were optimized to make approximations with $R^2 > 0.98$. Despite the complex and nonlinear transport mechanism, the CNN predicted for unseen Cu-CNT networks of various CNT volume fractions and Cu-CNT interfacial resistances with the R^2 greater than 98%. To provide a variety of learnable examples in CNN without performing additional FEM simulations, a simple image augmentation technique was used to diversify the training dataset by 4-folds. A possible extension of this work is to investigate the potential of CNN or other deep learning methods as rapid prediction models for microscopic images of fabricated bulk-scale Cu-CNT networks or other composite materials.

Data availability

The data included in this study is available from the corresponding author upon request as needed.

Received: 20 May 2022; Accepted: 18 July 2022

Published online: 10 August 2022

References

- Sundaram, R. M., Sekiguchi, A., Sekiya, M., Yamada, T. & Hata, K. Copper/carbon nanotube composites: Research trends and outlook. *R. Soc. Open Sci.* **5**, 180814 (2018).
- Krizhevsky, B. A., Sutskever, I. & Hinton, G. E. ImageNet classification with deep convolutional neural networks. *Commun. ACM* **60**, 84–90 (2012).

3. Mikolov, T., Deoras, A., Povey, D., Burget, L. & Černocký, J. Strategies for training large scale neural network language models. in *2011 IEEE Work. Autom. Speech Recognit. Understanding, ASRU 2011, Proc.* 196–201 (2011).
4. Kang, M. & Kwon, B. Deep learning of forced convection heat transfer. *J. Heat Transfer* **144**, 1–7 (2022).
5. Raissi, M., Yazdani, A. & Karniadakis, G. E. Hidden fluid mechanics: Learning velocity and pressure fields from flow visualizations. *Science* **367**, 1026–1030 (2020).
6. Edalatfar, M., Tavakoli, M. B., Ghalambaz, M. & Setoudeh, F. Using deep learning to learn physics of conduction heat transfer. *J. Therm. Anal. Calorim.* **146**, 1435–1452 (2021).
7. Yang, L., Dai, W., Rao, Y. & Chyu, M. K. Optimization of the hole distribution of an effusively cooled surface facing non-uniform incoming temperature using deep learning approaches. *Int. J. Heat Mass Transf.* **145**, 118749 (2019).
8. Kwon, B., Ejaz, F. & Hwang, L. K. Machine learning for heat transfer correlations. *Int. Commun. Heat Mass Transf.* **116**, 104694 (2020).
9. Wei, H., Zhao, S., Rong, Q. & Bao, H. Predicting the effective thermal conductivities of composite materials and porous media by machine learning methods. *Int. J. Heat Mass Transf.* **127**, 908–916 (2018).
10. Lee, K. W., Son, H. S., Cho, K. S. & Choi, H. J. Effect of interfacial bridging atoms on the strength of Al/CNT composites: Machine-learning-based prediction and experimental validation. *J. Mater. Res. Technol.* **17**, 1770–1776 (2022).
11. Matos, M. A. S., Pinho, S. T. & Tagarielli, V. L. Application of machine learning to predict the multiaxial strain-sensing response of CNT-polymer composites. *Carbon N. Y.* **146**, 265–275 (2019).
12. Le, T. T. Prediction of tensile strength of polymer carbon nanotube composites using practical machine learning method. *J. Compos. Mater.* **55**, 787–811 (2021).
13. Ejaz, F., *et al.* A two-dimensional finite element model for Cu-CNT composite: the impact of interface resistances on electrical and thermal transports. *Materilia* **24**, 101505 (2022).
14. Khaleghi, E., Torikachvili, M., Meyers, M. A. & Olevsky, E. A. Magnetic enhancement of thermal conductivity in copper-carbon nanotube composites produced by electroless plating, freeze drying, and spark plasma sintering. *Mater. Lett.* **79**, 256–258 (2012).
15. Choi, E. S. *et al.* Enhancement of thermal and electrical properties of carbon nanotube polymer composites by magnetic field processing. *J. Appl. Phys.* **94**, 6034–6039 (2003).
16. Dai, J., Wang, Q., Li, W., Wei, Z. & Xu, G. Properties of well aligned SWNT modified poly (methyl methacrylate) nanocomposites. *Mater. Lett.* **61**, 27–29 (2007).
17. Wang, Q., Dai, J., Li, W., Wei, Z. & Jiang, J. The effects of CNT alignment on electrical conductivity and mechanical properties of SWNT/epoxy nanocomposites. *Compos. Sci. Technol.* **68**, 1644–1648 (2008).
18. Zhou, B. *et al.* Thermal conductivity of aligned CNT/polymer composites using mesoscopic simulation. *Compos. Part A Appl. Sci. Manuf.* **90**, 410–416 (2016).
19. Ren, S., He, K., Girshick, R. & Sun, J. Faster R-CNN: Towards real-time object detection with region proposal networks. *IEEE Trans. Pattern Anal. Mach. Intell.* **39**, 1137–1149 (2017).
20. Russakovsky, O. *et al.* ImageNet large scale visual recognition challenge. *Int. J. Comput. Vis.* **115**, 211–252 (2015).
21. He, K., Zhang, X., Ren, S. & Sun, J. Deep residual learning for image recognition. in *Proc. IEEE Comput. Soc. Conf. Comput. Vis. Pattern Recognit.* **2016-December**, 770–778 (2016).
22. LeCun, Y., Bottou, L., Bengio, Y. & Haffner, P. Gradient-based learning applied to document recognition. *Proc. IEEE* **86**, 2278–2323 (1998).
23. Günen, M. A. Performance comparison of deep learning and machine learning methods in determining wetland water areas using EuroSAT dataset. *Environ. Sci. Pollut. Res.* **29**, 21092–21106 (2022).
24. Subramaniam, C. *et al.* One hundred fold increase in current carrying capacity in a carbon nanotube-copper composite. *Nat. Commun.* **4**, 1–7 (2013).
25. Akbarpour, M. R., Mousa Mirabad, H., Alipour, S. & Kim, H. S. Enhanced tensile properties and electrical conductivity of Cu-CNT nanocomposites processed via the combination of flake powder metallurgy and high pressure torsion methods. *Mater. Sci. Eng. A* **773**, 138888 (2020).
26. Pan, Y. *et al.* Fabrication, mechanical properties and electrical conductivity of Al₂O₃ reinforced Cu/CNTs composites. *J. Alloys Compd.* **782**, 1015–1023 (2019).
27. Daoush, W. M., Lim, B. K., Mo, C. B., Nam, D. H. & Hong, S. H. Electrical and mechanical properties of carbon nanotube reinforced copper nanocomposites fabricated by electroless deposition process. *Mater. Sci. Eng. A* **513–514**, 247–253 (2009).
28. Subramaniam, C. *et al.* Carbon nanotube-copper exhibiting metal-like thermal conductivity and silicon-like thermal expansion for efficient cooling of electronics. *Nanoscale* **6**, 2669–2674 (2014).
29. Chu, K. *et al.* Thermal properties of carbon nanotube-copper composites for thermal management applications. *Nanoscale Res. Lett.* **5**, 868–874 (2010).
30. Kim, K. T. *et al.* Influence of embedded-carbon nanotubes on the thermal properties of copper matrix nanocomposites processed by molecular-level mixing. *Scr. Mater.* **64**, 181–184 (2011).
31. Nie, J. H. *et al.* Fabrication and thermal conductivity of copper matrix composites reinforced by tungsten-coated carbon nanotubes. *Int. J. Miner. Metall. Mater.* **19**, 446–452 (2012).

Acknowledgements

This work was supported by a Grant from the Korea Institute of Science and Technology (KIST) Institutional Programs (2Z06541). D.S.L. acknowledges the support from the National Research Foundation of Korea (NRF-2017M3A7B4049167). J.S. acknowledges the support from the National Research Council of Science & Technology (NST) Grant by the Korea Government (MSIT) (No. CRC-20-01-NFRI).

Author contributions

F.E. conducted the electrical and thermal simulations, trained the ML models, analyzed the results, and wrote the first draft of the manuscript. L.K.H., J.S., J.-S. K. D.S.L. contributed to the ML methods and application, analyzed the results, and edited the manuscript. B.K. was the principal investigator of the research, designed the research, analyzed the results, and edited the manuscript.

Competing interests

The authors declare no competing interests.

Additional information

Correspondence and requests for materials should be addressed to B.K.

Reprints and permissions information is available at www.nature.com/reprints.

Publisher's note Springer Nature remains neutral with regard to jurisdictional claims in published maps and institutional affiliations.



Open Access This article is licensed under a Creative Commons Attribution 4.0 International License, which permits use, sharing, adaptation, distribution and reproduction in any medium or format, as long as you give appropriate credit to the original author(s) and the source, provide a link to the Creative Commons licence, and indicate if changes were made. The images or other third party material in this article are included in the article's Creative Commons licence, unless indicated otherwise in a credit line to the material. If material is not included in the article's Creative Commons licence and your intended use is not permitted by statutory regulation or exceeds the permitted use, you will need to obtain permission directly from the copyright holder. To view a copy of this licence, visit <http://creativecommons.org/licenses/by/4.0/>.

© The Author(s) 2022